Human Cranium Dynamic Analysis

Bo Wun Huang[1], Huang Kuang Kung[1], Kuan-Yu Chang[2], Po Kai Hsu[1], Jung-Ge Tseng[1*]

1 Graduate Institute of Mechatronics Engineering, Cheng Shiu University, Kaohsiung 833, Taiwan, R.O.C. 2 Mackay Memorial Hospital Taitung Branch, Taitung, Taiwan, ROC

Received November 20, 2009

Abstract: More and more brain related illnesses such as brain tumor, cerebral hemorrhage, nasopharyngeal carcinoma, cerebral artery/vein deformity, Parkinson's disease, epilepsy, etc., can be treated through skull surgery. However, the current automation technology of craniotomy is not matured and depends on physician's personal experience and technique. It is necessary to improve the operational security and success rate by fully understand the characteristic of cranium. This research investigates the dynamic property of cranium by experimental and theoretical analysis through skull model made in polystyrene. Reverse engineering analysis is adopted to build up geometric 3D skull CAD (Computer Aided Design) model. FEA (Finite element analysis) is conducted by transferring this 3D skull CAD model into ANSYS (FEA package) acceptable model. Experimental vibration measurement is obtained for the polystyrene skull model and the first few measured natural frequencies are obtained. Measured damping feature of the cranium model is discussed as well and together with other dynamic characteristics to provide complete information about the skull for medical doctor reference. [Life Science Journal. 2009; 6(4): 15– 22] (ISSN: 1097 – 8135)

Keywords Cranium vibration; dynamic characteristic; natural frequency; reverse engineering; brain related illness.

1. Introduction

Cranium is the hardest part and protects the most important part, brain – the commanding center, of human beings. Cranial neurosurgery need to treat patients suffering from brain lesions, traumatic brain injury (TBI), stroke, brain neuroglia tumor, cerebral hemorrhage, nasopharyngeal carcinoma, cerebral artery/vein deformity, etc., via craniotomy process. This treatment paradigm is costly, carries the risks associated with infection, additional surgery, and may cause cosmetic deformities. Owing to fast development of microsurgery, robotics are largely used in skull base surgery [1], minimally invasive surgery (a local anaesthetic, smaller cut, shorter operation time) becomes trend of brain surgery which allow doctors to remove the tumor, stop cerebral hemorrhage, and also surgically implant deep brain stimulators for the treatment of Parkinson's disease, epilepsy and cerebellar tremor. The procedure is also widely used in neuroscience for extracellular recording, brain imaging, and for neurological manipulations such as electrical stimulation and chemical titration. There exist high risks for the patient when proceeding brain surgery no matter how advanced the technology is [2]. The craniotomy is still one of the most complicate and difficult surgery. It is suggested to reduce the risk as much as possible by fully understanding the dynamic characteristic of human cranium for selecting the best surgery method, position, and cutting parameter of the skull.

Khalil et al.[3] conduct an experimental investigation to identify the resonance frequencies of two kinds of freely vibrating human dry skulls and extrapolate their results to living skulls taking into account of known and estimated differences in mechanical properties. Hakansson et al. [4] investigate of the free damped natural frequencies of human skull in vivo and damping coefficient is reported. Charalambopoulos et al. [5] deal with the free vibrations of the 3D viscoelastic human skull. Brantberg et al. [6] investigate the mechanisms for skull tap induced vestibular evoked myogenic potentials (VEMP) and found that skull tapping causes both skull vibration and head acceleration.

Yue et al. [7] analyze the strain of the thin-walled shell by the stress-strain calculation of a human skull with changing ICP (Intracranial pressure). Many patients exhibit excessive localized wear and tear of the

*Correspondence: james.tseng@csu.edu.tw
Dr. Bo Wun Huang

temporomandibular joint, due to the forces that develop in the human joint during function exceed tissue tolerance. Hashimoto and Clark [8] conduct experimental measurement of vibration transmission between the cranium and mandible in healthy humans during variations of jaw position. Kerr and Adams [9] find out cranial base and jaw relationship. Several papers [10~12] discuss endodontic evaluation, facial types, facial relationships, respectively. [10~12]

Lin and Tsai [13] address a method to construct 3D finite element model by using PA (Posterior to Anterior) view and lateral view of cephalographs to compensate the deficient traditional cephalometry analysis. Su and Chang analyze the stresses in post-restored teeth by finite element method and the variables evaluated were loading modes, shapes, diameters, materials of the posts. Similar approach has been down by others. [14~16]

The purpose of this research is to find basic dynamic characteristic of human cranium such as natural frequencies, damping ratios, mode shapes, etc. and to increase the success rate during skull surgery. Reverse engineering is performed to obtain computer 3D diagram of the polystyrene skull model. This computer 3D model is then fed into ANSYS FEM (Finite Element Method) software [17] to carry out dynamic analysis. First few fundamental natural frequencies were measured by vibration test and compared with FEM results.

2. Reverse engineering (RE) nite element analysis

As computer-aided design (CAD) has become more popular, reverse engineering (RE) has become a viable method to create a 3D virtual model of an existing physical part for use in 3D CAD, CAM, CAE or other software.[18] The reverse-engineering process involves measuring an object, reconstructing it as a 3D model, manufacturing the mold and product. The physical object can be measured using 3D scanning technologies like CMMs (Coordinate Measuring Machine), laser scanners, structured light digitizers or computed tomography. The measured data alone, usually represented as a point cloud, lacks topological information and is therefore often processed and modeled into a more usable format such as a triangular-faced mesh, a set of NURBS surfaces or a CAD model. Reverse engineering is also used by businesses to bring existing physical geometry into digital product development environments, to make a digital 3D record of their own products or to assess competitors' products. It is used to analyze, for instance, how a product works, what it does, and what components it consists of, estimate costs, and identify potential patent infringement, etc.

A low error, fast measuring speed, non-contact laser scanner, the ATOS optical measuring machine manufactured by GOM, Germany (shown in Figure 1), is adopted to measure the complex 3D profile of polystyrene skull model (shown in Figure 2).

Figure 1. ATOS non-contact laser scanning system

Figure 2. Polystyrene skull model

The ATOS system is composed by an optical grating projector and two industrial CCD cameras. It digitizes three dimensional work pieces by projecting a grid onto the part and using two cameras, in two different positions, at two different angles with respect to the work piece to triangulate the location of the intersection points on the grid. The point locations triangulated by the

ATOS system may then be stored as a point cloud (over half million points) and may also be transformed into facet bodies, such as STL polygon meshes, by software components supplied by GOM or third party. The resulting STL diagram from ATOS system which reconstructs the complex 3D cranium model in electronic file is shown in Fig. 3.

Figure 3. 3D Computer cranium model reconstructed by ATOS system

3. Finite element analysis

3.1. Fundamental theory

The equation of motion of the skull can be derived via finite element method by apply Lagrange equation as follows:

$$\frac{d}{dt}\left(\frac{\partial L}{\partial \dot{\vec{Q}}}\right)-\left(\frac{\partial L}{\partial \vec{Q}}\right)+\left(\frac{\partial R}{\partial \dot{\vec{Q}}}\right)=\{0\} \qquad (1)$$

where, L=T-V is Lagrange function, T and V are kinetic and potential energy of the skull model, respectively. R is dissipation function. $\vec{Q}$ and $\dot{\vec{Q}}$ represent displacement and velocity of the skull model. The discretized equation of motion of the skull structure is:

$$[M]\,\ddot{\vec{Q}}(t)+[C]\,\dot{\vec{Q}}(t)+[K]\,\vec{Q}(t)=\vec{P}(t) \qquad (2)$$

where, $\ddot{\vec{Q}}$ is the acceleration vector of the node of skull model. For an undamped, no external force linear system, the equation of motion becomes:

$$[M]\,\ddot{\vec{Q}}(t)+[K]\,\vec{Q}(t)=0. \qquad (3)$$

The displacement of this linear undamped linear system is in the complex plane and can be assumed as follows:

$$\vec{Q}=\{\phi\}e^{i\omega t} \qquad (4)$$

where, $\{\phi\}$ and ω are the mode shapes and the natural frequencies of the skull structure, respectively. Substitute equation (4) into equation (3), one can get:

$$(-\omega^2[M]+[K])\{\phi\}=0. \qquad (5)$$

Solve for the eigenvalue and eigenvector in equation (5) can get natural frequencies ω and displacement vectors (mode shapes) $\{\phi\}$ of the skull structure.

3.2. FE model establishment and analysis

The reconstructed 3D Computer cranium model by ATOS system is imported into ANSYS FE software to build up the FE model. Standard procedure is followed to select elements, cut off elements, set up material properties (shown in Table 1) and boundary conditions, etc. Around 120,000 elements are built and the full scale 3D skull FE model is shown in Figure 4.

Table 1. Material property of Polystyrene

Material property	value
Young's modulus	1.14 GPa
Density	1,380 Kg/m^3
Poisson's ratio	0.3

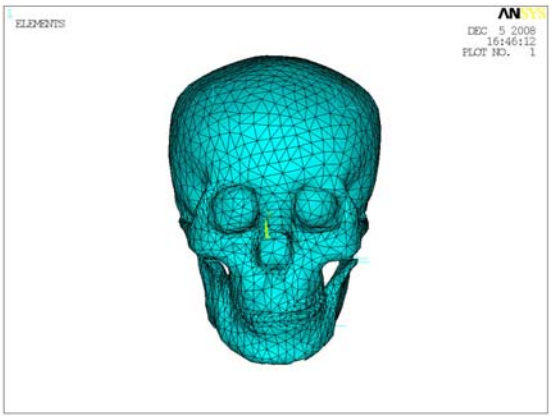

Figure 4. 3D FE model with around 120,000 elements

Before go into detail of analysis, the element numbers convergence test has been done and 100,000

elements are sufficient and used for carry out the full scale vibration analysis for the 3D skull system. First four modes of the skull system are observed from the ANSYS results and their degenerated natural frequencies are around 1500 Hz (shown in Table 2) with different mode shapes as shown in Figure 5 ~ Figure 8.

Table 2. First four theoretical frequencies of skull model

Frequencies / Mode	Hz
First mode	1,500
Second mode	1,500
Third mode	1,501
Fourth mode	1,501

Note that the fourth mode shape shown in Fig. 8 has vibration amplitude on the back of the skull so it can not be seen clearly at front view.

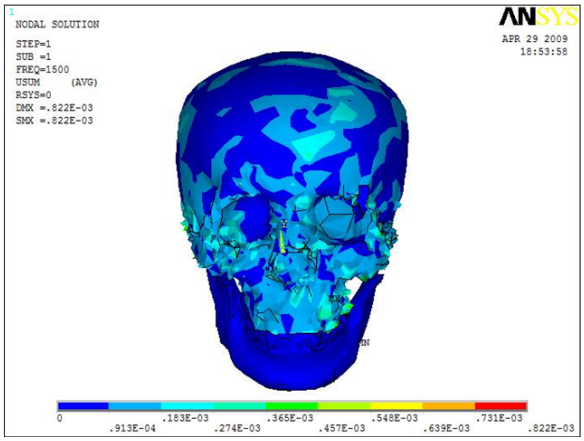

Figure 5. First mode of 3D skull model

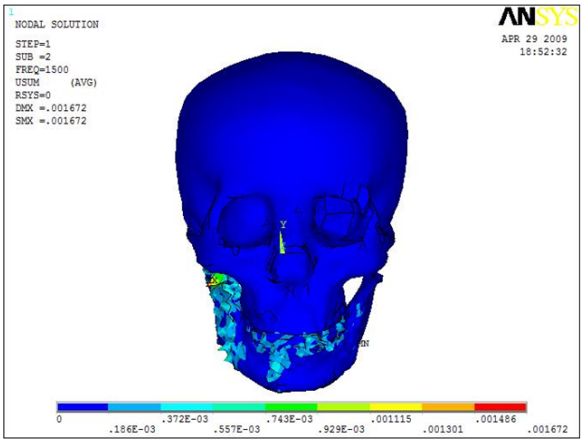

Figure 6. Second mode of 3D skull model

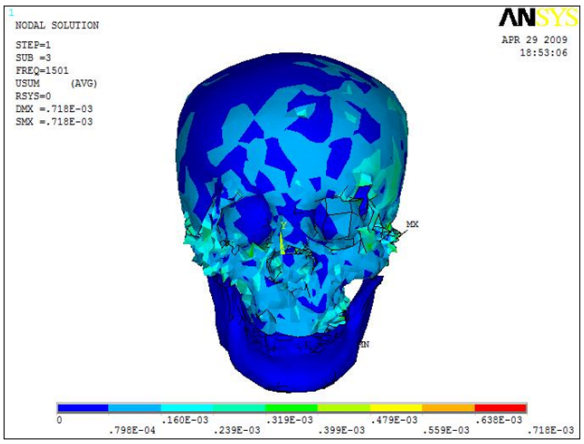

Figure 7. Third mode of 3D skull model

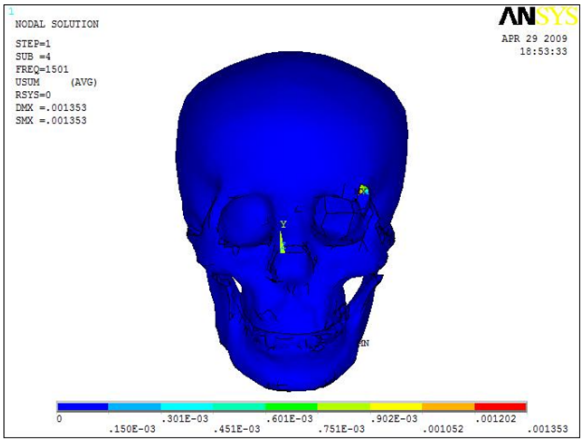

Figure 8. Fourth mode of 3D skull model

4. Experimental analysis

The experimental set up is shown in Fig. 9 to measure the vibration frequency, time response, and damping ratio, etc. for the Polystyrene skull model. The skull model is fixed at the center near cerebellum position. An impact hammer and an accelerometer are connected to channel 1 and 2, respectively, of HP 35670A spectrum analyzer. The impact hammer hits on different positions: top, front, back, right, and left of the Polystyrene skull model in sequence during the measurement and the micro accelerometer is fixed on the top of the skull. Combine the hammer's input signal with the micro accelerometer's output response signal of the Polystyrene skull model, the natural frequencies and time responses are obtained by HP analyzer. The frequency

spectrums when the impact hammer is hitting on top, right, and back of the Polystyrene skull model are shown in Fig. 10~12. The measured fundamental frequencies are 1,410 Hz, 1,790 Hz, 1,888 Hz, 1,984 Hz, 2,320 Hz, 3,792 Hz, etc., as shown in Table 3.

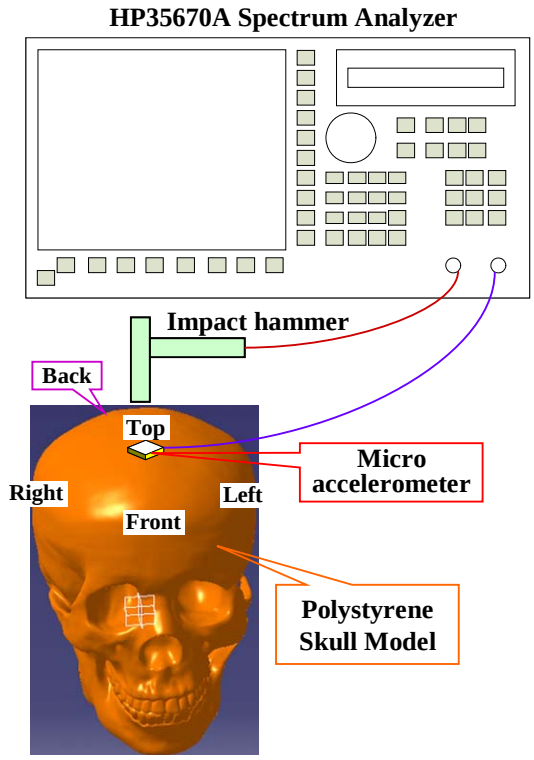

Figure 9. Experimental set up of the Polystyrene skull model

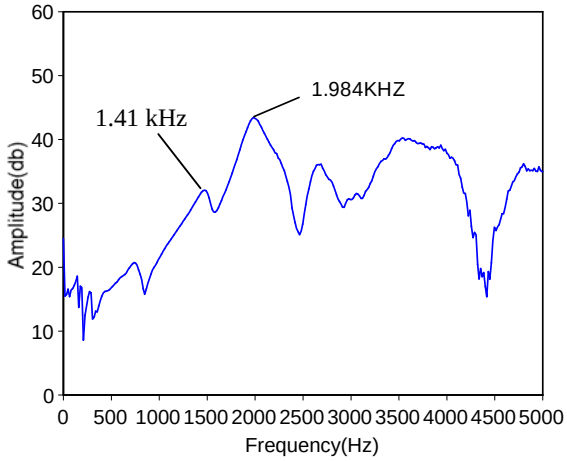

Figure 10. Frequency spectrum when hits on the top of the skull model

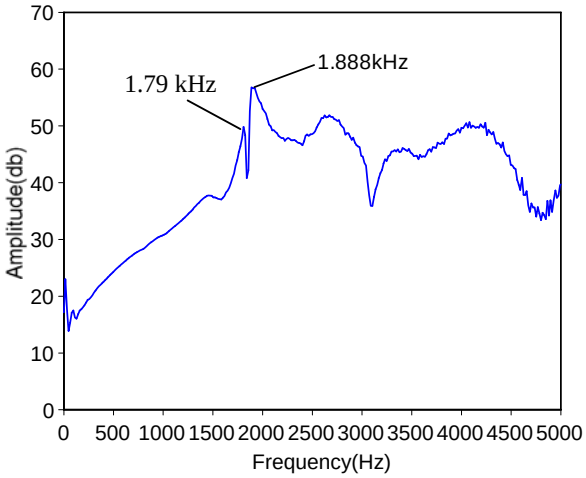

Figure 11. Frequency spectrum when hits on the right of the skull model

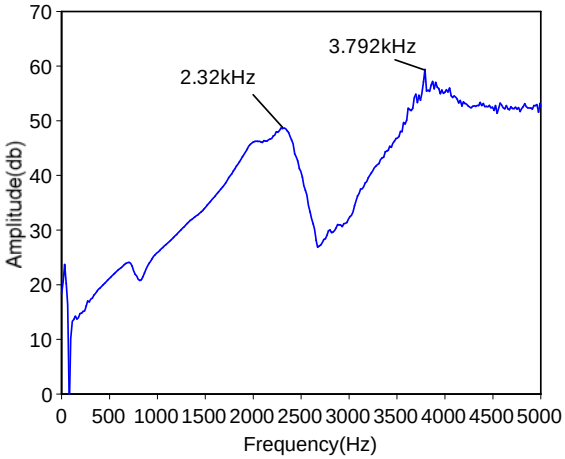

Figure 12. Frequency spectrum when hits on the back of the skull model

Table 3. First six measured frequencies of skull model

Mode \ Frequencies	Hz
First mode	1,410
Second mode	1,790
Third mode	1,888
Fourth mode	1,984
Fifth mode	2,320
sixth mode	3,792

These spectrum figures (Figures 10~12) indicate when hit on different positions, some frequencies will show up and some don't due to complicated distribution

of the nodal lines or circles on the 3D skull model. In other words, when the input excitation or output response points are on or very near to a nodal line or circle, the specific mode will be suppressed and can not shown as a peak value in the frequency spectrum. Therefore the purpose of hitting different positions of the skull is to find as much modes as possible for a complete experimental result.

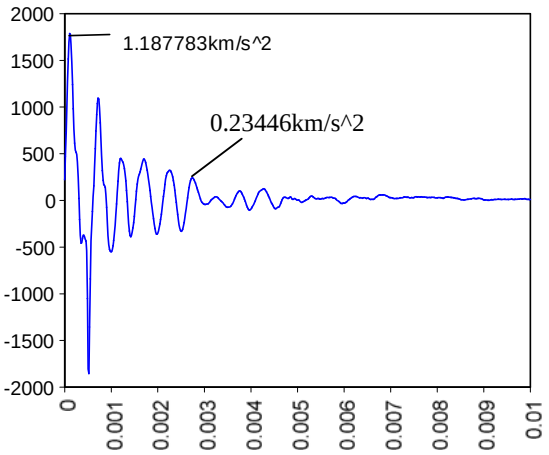

Figure 13. Time response when hits on the top of the skull model

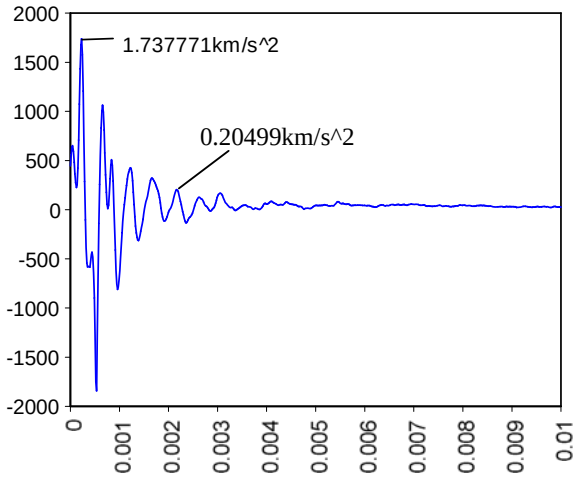

Figure 14. Time response when hits on the back of the skull model

Measured time responses are obtained for the impact hammer hits on different positions: top, front, back, right, and left of the polystyrene skull model in sequence while accelerometer fixed on the top of the skull model. The time responses when impact hammer hits on the top and back are shown in Fig. 13 and Fig. 14.

5. Discussion

The FEM analyzed and measured fundamental frequency of the skull is compared in Table 4. It can be seen that the FEM analyzed and measured first frequency are 1500 Hz and 1410 Hz, respectively. The errors between them are about 6.4% and falls into practical acceptable range between theoretical predict and experimental results.

Table 4. Comparison between FEM analyzed and measured fundamental frequency of skull model

Mode / Frequency	First mode
FEM analyzed (Hz)	1500
Measured (Hz)	1410
Error (%)	6.4%

Damping ratio (ζ) of the polystyrene skull model can be obtained by employing the following equation:

$$\zeta = \frac{\delta}{\sqrt{(2\pi)^2 + \delta^2}} \tag{6}$$

where $\delta = \frac{1}{m}\ln\left\{\frac{X_1}{X_{m+1}}\right\}$. X_1 is the first peak and X_{m+1} is the $(m+1)^{th}$ peak in time response diagram, m is an integer and represents the number of cycle times.

By substituting X_1=1.188, X_{m+1}=0.2345, m=5, etc., from Fig. 13, into equation (6), the measured damping ratios ζ_1 = 0.051. Similarly, by substituting X_1=1.738, X_{m+1}=0.205, m=5, etc., from Fig. 14, into equation (6), the measured damping ratios ζ_2 = 0.055. All six time responses obtain from different hitting position by the impact hammer are calculated in the same manner and the average damping ratio of the skull is ζ_{avg} = 0.053.

6. Summary

This research investigates the dynamic characteristic of a polystyrene skull model. The aim for this research field is to understand the vibration phenomena of the polystyrene first and then use this model to analyze the normal modes and related

parameters of real human cranium in the future. Therefore, the result of this research is quite useful for physician's reference.

Several aspects are discovered during this research and listed as follows:

1. Reverse engineering is a very useful and effective way to rebuild a 3D complex geometry and allow the researchers to continue proceeding with the real analysis work.
2. FE analysis is performed according to the large amount of geometric data point obtained from ATOS system. The error between the first natural frequency of the polystyrene skull model obtained from both FEM solution and measurement is about 6.4%. The promising result shows that the approach model proposed by this paper is on the right track and can be further expanding of its usage.
3. Measurements of different positions in the experiment is a necessary procedure to find out complete natural frequencies in the spectrum.

Acknowledgements

This work was coworked with Dr. Wang in xx hospital and finished in Vibration and Noise Laboratory Cheng Shiu University. The author would like to thank the National Science Council, Taiwan, Republic of China, for financially supporting this research through Grant NSC95-2212-E-230-006.

References

1. B. Plinkert, P.K. Plinkert, Robotics in skull base surgery, International Congress Series, 2001, 1230: 138–142.
2. Melville J. Da Cruz, Paul Fagan, MD, Marcus Atlas, and Celene McNeill, Drill induced hearing lost in the nonoperative ear, Otolaryngology- Head and Neck Surgery, 1997, 117:555-558.
3. T. B. Khalil, D. C. Viano, D. L. Smith, Experimental analysis of the vibrational characteristics of the human skull, Journal of Sound and Vibration, 1979, 63 (3): 351-376.
4. B. Håkansson, A. Brandt and P. Carlsson, Resonance frequencies of the human skull in vivo, Journal of Acoustic Society of America, 1994, 95 (3):1474–1481.
5. A. Charalambopoulos, D. I. Fotiadis, C. V. Massalas, Free vibrations of the viscoelastic human skull, International Journal of Engineering Science, 1998, 36 (5/6): 565-576.
6. Krister Brantberg, Lennart Löfqvist, Magnus Westin, Arne Tribukait, Skull tap induced vestibular evoked myogenic potentials: An ipsilateral vibration response and a bilateral head acceleration response? Clinical Neurophysiology, 2008, 119:2363–2369.
7. Xianfang Yue, Li Wang, Feng Zhou, Amendment on the strain measurement of thin-walled human skull shell as intracranial pressure changes, Journal of University of Science and Technology BeiJing, 2008, 15 (2):202-208.
8. Kazuyoshi Hashimoto, Glenn T. Clark, The effect of altering jaw position on the transmission of vibration between the skull and teeth in humans, Archives of Oral Biology, 2001, 46:1031–1038.
9. W. J. S. Kerr and C.P. Adams, Cranial base and jaw relationship", American Journal of Physical Anthropology, 1998, 77:213-220.
10. Kuo-Chih Su, Chih Han Chang, Biomechanical evaluation endodontic posts-finite element analysis, 2006. Master Thesis, National Cheng Kung University, Tainan, Taiwan, R.O.C.
11. V. A. Sassouni, A classification of skeletal facial types, American Journal of Orthodontics and Dentofacial Orthopedics, 1969, 55: 109-123.
12. W. B.Downs, Variations in facial relationships: their significance in treatment and prognosis, American Journal of Orthodontics and Dentofacial Orthopedics, 1948, 34: 812.
13. Chi Shiun Lin, Chin Chong Tsai, The morphological research on the construction of mandible finite element model using 2D cephalomatric images, Master Thesis, Tunghai University, 2004.
14. B. H. Grayson, N. Weintraub, F. L. Bookstein, and J. G. McCarty, A Comparative Cephalometric Study of the Cranial Base in the Craniofacial Anomalies: Part I: Tensor Analysis. Cleft Palate Craniofacial Journal, 1985, 22: 75-86.

15. A. F. Ayoub, Strirrups Dr., The practicability of finite-element analysis for assessing changes in human craniofacial morphology from cephalograph, Archives of Oral Biology, 1993, 38: 679-683.

16. G. D. Singh, J. A. Jr. McNamara and S. Lozanoff, Thin-plate spline analysis of the cranial base in subjects with class III malocclusion, European Journal of Orthodontics, 1997, 19:341-353.

17. Huang Kuang Kung, Bo Wun Huang, Hung Shiung Chen, ANSYS and Computer Aided Engineering Analysis, 2004, Cheng Shiu University, Kaohsiung, Taiwan, R.O.C.

18. Chong-Ching Chang, Reverse engineering and the integration application, 1999, Gau Lih Book Co. Ltd., ISBN 957-584-664-8.